

## Spectroscopic Characterization of a Series of Platinum Acetylide Complexes Having a Localized Triplet Exciton

Thomas M. Cooper,<sup>\*,†</sup> Douglas M. Krein,<sup>†,‡</sup> Aaron R. Burke,<sup>†,‡</sup> Daniel G. McLean,<sup>†,§</sup> Joy E. Rogers,<sup>†,||</sup> Jonathan E. Slagle,<sup>†,⊥</sup> and Paul A. Fleitz<sup>†</sup>

Materials and Manufacturing Directorate, Air Force Research Laboratory, Wright-Patterson Air Force Base, Ohio 45433, Anteon Corporation, Dayton, Ohio 45431, SAIC, Dayton, Ohio 45434, UES, Inc., Dayton, Ohio 45432, and AT&T Corporation, Dayton, Ohio 45434

Received: November 17, 2005; In Final Form: February 13, 2006

In this work, we describe the spectroscopic properties of a series of platinum complexes containing one acetylide ligand per platinum, having the chemical formula *trans*-Pt(PBu<sub>3</sub>)<sub>2</sub>((C≡CC<sub>6</sub>H<sub>4</sub>)<sub>n</sub>-H)Cl, *n* = 1–3 (designated as **half-PEn-Pt**) and compare their spectroscopic behavior with the well-characterized series *trans*-Pt(PBu<sub>3</sub>)<sub>2</sub>((C≡CC<sub>6</sub>H<sub>4</sub>)<sub>n</sub>-H)<sub>2</sub>, *n* = 1–3 (designated as **PEn-Pt**). This comparison aims to determine if the triplet state of **PEn-Pt** is confined to one ligand or delocalized across the central platinum atom. We measured ground-state absorption spectra, fluorescence spectra, phosphorescence spectra, and triplet-state absorption spectra. The ground-state absorption spectra and fluorescence spectra both showed a blue shift when comparing **half-PEn-Pt** with **PEn-Pt**, showing the S<sub>1</sub> state is delocalized across the platinum. In contrast, the phosphorescence spectra of the two types of compounds had the same 0–0 band energy, showing the T<sub>1</sub> state was confined to one ligand in **PEn-Pt**. The triplet state absorption spectra blue shifted when comparing **half-PEn-Pt** with **PEn-Pt**, showing the T<sub>n</sub> state was delocalized across the central platinum. This comparison supports recently published work that suggested this confinement effect (Rogers, J. E et al. *J. Chem. Phys.* 2005, 122, 214701).

### Introduction

Platinum acetylide complexes are good systems to probe triplet-state phenomena like ground-state absorption to the triplet state (S<sub>0</sub>→T<sub>1</sub>), intersystem crossing (S<sub>1</sub>→T<sub>1</sub>), triplet-state absorption spectrum (T<sub>1</sub>→T<sub>n</sub>), and phosphorescence (T<sub>1</sub>→S<sub>0</sub>).<sup>1,2</sup> In our group, we have been investigating the relation between chemical structure and spectroscopic properties in platinum acetylide complexes such as *trans*-Pt(II)(PBu<sub>3</sub>)<sub>2</sub>((C≡CC<sub>6</sub>H<sub>4</sub>)<sub>n</sub>-H)<sub>2</sub>, where *n* = 1–3.<sup>3–5</sup> An issue that has been investigated by our group as well as other groups is the relation between molecular structure and the delocalization of the singlet and triplet excitons. A theoretical and experimental investigation of the polymer poly(Pt(PBu<sub>3</sub>)<sub>2</sub>(C≡CC<sub>6</sub>H<sub>4</sub>)) finds the triplet exciton T<sub>1</sub> is localized on a single phenylene ring while the S<sub>1</sub> and T<sub>n</sub> excitons are delocalized over several monomer units.<sup>6</sup> More recently, a series of oligomers having the formula C<sub>6</sub>H<sub>5</sub>(C≡C-Pt(PBu<sub>3</sub>)<sub>2</sub>-C≡CC<sub>6</sub>H<sub>4</sub>)<sub>n</sub>-H, *n* = 1–5, 7 has been prepared.<sup>7</sup> The ground-state absorption and fluorescence spectra show systematic red shifts as the oligomer length increases. In contrast, the phosphorescence spectra show only small red shifts with increasing oligomer length. The results support the idea that the triplet state is more localized than the singlet state. An investigation of the photophysics and photochemistry of platinum acetylide stilbenes gives evidence that triplet state resides

on one ligand.<sup>8</sup> In our group, we measured time-resolved infrared spectra of the triplet state *trans*-Pt(PBu<sub>3</sub>)<sub>2</sub>((C≡C-C<sub>6</sub>H<sub>4</sub>-C≡CC<sub>6</sub>H<sub>5</sub>)<sub>2</sub>).<sup>9</sup> We also did density functional theory calculations of the S<sub>0</sub> and T<sub>1</sub> state and found the S<sub>0</sub> state contains contributions from Pt 5d and ligand π orbitals. The T<sub>1</sub> state contains only contributions from ligand π\* orbitals. From symmetry considerations, the calculations predict the triplet state will reside on both ligands. A related time-resolved infrared spectroscopy and theoretical study suggests the triplet exciton is confined to one ligand.<sup>10</sup> In another study, the intervalence charge-transfer bands of a monocationic diphenylamino-substituted platinum acetylide complex is compared with a model compound.<sup>11</sup> They conclude the platinum atom has only a small effect on the electronic delocalization of the molecule. To help resolve these issues, we recently published a detailed investigation of the photophysical properties of a series of butadiynes having the formula H-(C<sub>6</sub>H<sub>4</sub>-C≡C)<sub>n</sub>-(C≡C-C<sub>6</sub>H<sub>4</sub>)<sub>n</sub>-H, *n* = 1–3 and ligands H-(C<sub>6</sub>H<sub>4</sub>-C≡C)<sub>n</sub>-H, *n* = 1–3 and compared these to previous work done on a complimentary series of platinum-containing complexes having the formula *trans*-Pt((P(C<sub>4</sub>H<sub>9</sub>)<sub>3</sub>)<sub>2</sub>((C≡C-C<sub>6</sub>H<sub>4</sub>)<sub>n</sub>-H)<sub>2</sub>, *n* = 1–3.<sup>5,12</sup> By analysis of the behavior of the singlet and triplet state with increasing molecular size, we found evidence that the singlet state is delocalized throughout the molecule but that the triplet state is confined to one ligand in the platinum complexes. Recently, another theoretical study also suggests the triplet state is confined to one ligand.<sup>13</sup>

In this work, we describe the synthesis and spectroscopic properties of a series of platinum complexes containing one acetylide ligand per platinum, having the chemical formula *trans*-Pt((PC<sub>4</sub>H<sub>9</sub>)<sub>3</sub>)<sub>2</sub>((C≡C-C<sub>6</sub>H<sub>4</sub>)<sub>n</sub>-H)Cl, *n* = 1–3 (designated as **half-PEn-Pt**) and compare their spectroscopic behavior with

\* To whom correspondence should be addressed. E-mail: Thomas.Cooper@wpafb.af.mil.

<sup>†</sup> Materials and Manufacturing Directorate, Air Force Research Laboratory, Wright-Patterson Air Force Base, OH 45433.

<sup>‡</sup> Anteon Corporation, Dayton, OH 45431.

<sup>§</sup> SAIC, Dayton, OH 45434.

<sup>||</sup> UES, Inc., Dayton, OH 45432.

<sup>⊥</sup> AT&T Corporation, Dayton, OH 45434.

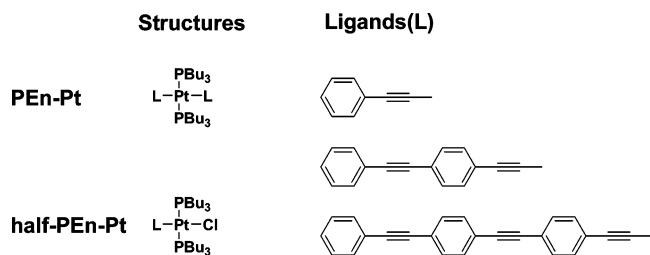


**Figure 1.** List of compounds discussed in this study.

the well-characterized series *trans*-Pt((PC<sub>4</sub>H<sub>9</sub>)<sub>3</sub>)<sub>2</sub>((C≡C-C<sub>6</sub>H<sub>4</sub>)<sub>n</sub>-H)<sub>2</sub>, *n* = 1–3 (designated as **PEn-Pt**) (Figure 1) The previous investigations<sup>5,12</sup> provide a baseline study with which it is possible to compare their spectroscopic behavior with the asymmetric complexes. This study is a direct measurement of the delocalization of the singlet and triplet excitons in platinum acetylide complexes. The results from this work show the singlet exciton of **PEn-Pt** complexes is delocalized across the platinum with contributions from both ligands, while the triplet exciton is confined to one ligand.

### General Synthesis Techniques

All reactions were carried out using dry, distilled solvents and under dry, high-purity nitrogen. All reagents were purchased from Aldrich Chemical Co. and used without further purification. Alumina column refers to a support of Al<sub>2</sub>O<sub>3</sub> (Activated, neutral, Brockman grade I, standard grade, ~150 mesh, 58 Å). Reverse-phase column refers to Alltech Extract-Clean C18. Microwave refers to CEM Inc. Discover System. The compounds Pt(C≡C-C<sub>6</sub>H<sub>5</sub>)<sub>2</sub>(PBu<sub>3</sub>)<sub>2</sub> (**PE1-Pt**), Pt(C≡C-C<sub>6</sub>H<sub>4</sub>-C≡C-C<sub>6</sub>H<sub>5</sub>)<sub>2</sub>(PBu<sub>3</sub>)<sub>2</sub> (**PE2-Pt**) and Pt(C≡C-C<sub>6</sub>H<sub>4</sub>-C≡C-C<sub>6</sub>H<sub>4</sub>-C≡C-C<sub>6</sub>H<sub>5</sub>)<sub>2</sub>(PBu<sub>3</sub>)<sub>2</sub> (**PE3-Pt**) were synthesized as described previously.<sup>5</sup>

### Synthesis

**PtCl(C≡C-C<sub>6</sub>H<sub>5</sub>)(PBu<sub>3</sub>)<sub>2</sub> (half-PE1-Pt).** A solution of PtCl<sub>2</sub>(PBu<sub>3</sub>)<sub>2</sub> (739 mg, 1.1 mmol) and C<sub>6</sub>H<sub>5</sub>C≡CH (102 mg, 1.0 mmol) in NHEt<sub>2</sub> (25 mL) and CuI (33 mg, 0.17 mmol) was heated in a microwave for 30 min at 115 °C. Solvent was removed and the yellow residue dissolved in CH<sub>2</sub>Cl<sub>2</sub> and filtered through an alumina plug. The residue was purified with reverse-phase chromatography, forming a yellow oil, identified as PtCl(C≡C-C<sub>6</sub>H<sub>5</sub>)(PBu<sub>3</sub>)<sub>2</sub> (407 mg, 55%). MA: found C, 52.09; H, 7.66%. C<sub>32</sub>H<sub>59</sub>ClP<sub>2</sub>Pt requires C, 52.20; H, 8.08%. *M*<sub>w</sub> = 736.29. IR: (KBr, thin film) 2119 cm<sup>-1</sup> ν(Pt-C≡C). <sup>1</sup>H NMR (CDCl<sub>3</sub>): δ 0.93 (m, 18H, CH<sub>3</sub>), 1.45 (m, 12H, CH<sub>2</sub>), 1.59 (m, 12H, CH<sub>2</sub>), 2.02 (m, 12H, CH<sub>2</sub>), 7.08–7.28 (m, 5H, ArH) ppm. <sup>13</sup>C NMR (CDCl<sub>3</sub>): δ 14.03 (s, CH<sub>3</sub>), 22.26 (t, *J*(CP) = 17 Hz, CH<sub>2</sub>), 24.55 (t, *J*(CP) = 7 Hz, CH<sub>2</sub>), 26.35 (s, CH<sub>2</sub>), 83.28 (t, *J*(CPT) = 14.6 Hz, Pt-C≡C), 101.28 (t, *J*(CPT) = 2.5 Hz, C≡C), 125.31, 128.10, 129.17, 130.9(Ar) ppm. <sup>31</sup>P NMR (CDCl<sub>3</sub>): δ 8.07 (s and d centered at δ8.07, *J*(PPt) = 2380 Hz, PBu<sub>3</sub>) ppm. EIMS: (*m/z*) 736.

**PtCl(C≡C-C<sub>6</sub>H<sub>4</sub>-C≡C-C<sub>6</sub>H<sub>5</sub>)(PBu<sub>3</sub>)<sub>2</sub> (half-PE2-Pt).** A solution of PtCl<sub>2</sub>(PBu<sub>3</sub>)<sub>2</sub> (748 mg, 1.1 mmol) and C<sub>6</sub>H<sub>5</sub>C≡C-C<sub>6</sub>H<sub>4</sub>C≡CH (203 mg, 1.0 mmol) in NHEt<sub>2</sub> (25 mL) and CuI (33 mg, 0.17 mmol) was heated in a microwave for 30 min at 115 °C. Solvent was removed and the yellow residue dissolved in CH<sub>2</sub>Cl<sub>2</sub> and filtered through an alumina plug. The residue was purified with reverse-phase chromatography, forming a yellow oil that slowly solidified, identified as PtCl(C≡C-C<sub>6</sub>H<sub>4</sub>-C≡C-C<sub>6</sub>H<sub>5</sub>)(PBu<sub>3</sub>)<sub>2</sub> (329 mg, 39%). MA: found C, 57.28; H, 7.50%. C<sub>40</sub>H<sub>63</sub>ClP<sub>2</sub>Pt requires C, 57.44; H, 7.59%,

*M*<sub>w</sub> = 836.41. IR: (KBr, thin film) 2114 cm<sup>-1</sup> ν(Pt-C≡C). <sup>1</sup>H NMR (CDCl<sub>3</sub>): δ 0.95 (m, 18H, CH<sub>3</sub>), 1.46 (m, 12H, CH<sub>2</sub>), 1.59 (m, 12H, CH<sub>2</sub>), 2.02 (m, 12H, CH<sub>2</sub>), 7.21–7.54 (m, 9H, ArH) ppm. <sup>13</sup>C NMR (CDCl<sub>3</sub>): δ 14.07 (s, CH<sub>3</sub>), 22.29 (t, *J*(CP) = 17 Hz, CH<sub>2</sub>), 24.58 (t, *J*(CP) = 7 Hz, CH<sub>2</sub>), 26.35 (s, CH<sub>2</sub>), 87.32 (t, *J*(CPT) = 14.3 Hz, Pt-C≡C), 101.61 (t, *J*(CPT) = 2.5 Hz, C≡C), 90.27 (s, C≡C), 90.19 (s, C≡C), 119.8, 123.8, 128.3, 128.6, 129.3, 130.9, 131.5, 131.7(Ar) ppm. <sup>31</sup>P NMR (CDCl<sub>3</sub>): δ 8.14 (s and d centered at δ8.14 *J*(PPt) = 2366 Hz, PBu<sub>3</sub>) ppm. EIMS: (*m/z*) 836.

**PtCl(C≡C-C<sub>6</sub>H<sub>4</sub>-C≡C-C<sub>6</sub>H<sub>4</sub>-C≡C-C<sub>6</sub>H<sub>5</sub>)(PBu<sub>3</sub>)<sub>2</sub> (half-PE3-Pt).** A solution of PtCl<sub>2</sub>(PBu<sub>3</sub>)<sub>2</sub> (755 mg, 1.1 mmol) and C<sub>6</sub>H<sub>5</sub>C≡C-C<sub>6</sub>H<sub>4</sub>C≡C-C<sub>6</sub>H<sub>4</sub>C≡CH (300 mg, 1.0 mmol) in NHEt<sub>2</sub> (25 mL) and CuI (20 mg, 0.17 mmol) was heated in a microwave for 30 min at 115 °C. Solvent was removed and the yellow residue dissolved in CH<sub>2</sub>Cl<sub>2</sub> and filtered through an alumina plug. The residue was purified with reverse-phase chromatography, forming a yellow solid, identified as PtCl(C≡C-C<sub>6</sub>H<sub>4</sub>C≡C-C<sub>6</sub>H<sub>4</sub>-C≡C-C<sub>6</sub>H<sub>5</sub>)(PBu<sub>3</sub>)<sub>2</sub> (365 mg, 39%). MA: found C, 61.28; H, 7.11%. C<sub>48</sub>H<sub>67</sub>ClP<sub>2</sub>Pt requires C, 61.56; H, 7.21%. *M*<sub>w</sub> = 936.52. IR: (KBr, thin film) 2113 cm<sup>-1</sup> ν(Pt-C≡C). <sup>1</sup>H NMR (CDCl<sub>3</sub>): δ 0.96 (m, 18H, CH<sub>3</sub>), 1.47 (m, 12H, CH<sub>2</sub>), 1.61 (m, 12H, CH<sub>2</sub>), 2.04 (m, 12H, CH<sub>2</sub>), 7.22–7.56 (m, 13H, ArH) ppm. <sup>13</sup>C NMR (CDCl<sub>3</sub>): δ 13.93 (s, CH<sub>3</sub>), 22.45 (t, *J*(CP) = 17 Hz, CH<sub>2</sub>), 24.58 (t, *J*(CP) = 7 Hz, CH<sub>2</sub>), 26.37 (s, CH<sub>2</sub>), 87.93 (t, *J*(CPT) = 14.3 Hz, Pt-C≡C), 101.72 (t, *J*(CPT) = 2.5 Hz, C≡C), 89.47 (s, C≡C), 90.01 (s, C≡C), 90.49 (s, C≡C), 92.18 (s, C≡C), 119.6, 123.2, 123.4, 123.7, 128.6, 128.8, 129.6, 130.9, 131.5, 131.7, 134.0(Ar) ppm. <sup>31</sup>P NMR (CDCl<sub>3</sub>): δ 8.26 (s and d centered at δ 8.26, *J*(PPt) = 2374 Hz, PBu<sub>3</sub>) ppm. EIMS: (*m/z*) 936.

### General Spectroscopy Techniques

All absorption and fluorescence spectra were obtained from benzene solutions. Ground-state UV/Vis absorption spectra were measured on a temperature-controlled Cary 500 spectrophotometer. Emission spectra at 5-nm slit width were measured using a Perkin-Elmer model LS 50B fluorometer. Low-temperature phosphorescence was done in methyltetrahydrofuran as a frozen glass at 77 K and exciting at 350 nm except **half-PE1-Pt** and **PE1-Pt**, which were excited at 325 nm. Nanosecond transient absorption measurements were carried out using the third and fourth harmonics (355 and 266 nm) of a Q-switched Nd:YAG laser (Quantel Brilliant, pulse width ca. 5 ns). All samples were deoxygenated with three freeze-pump-thaw cycles. Pulse fluences of up to 8 mJ cm<sup>-2</sup> are typically used at the excitation wavelength. Ground-state absorption spectra were obtained before and after the flash photolysis experiment. Most samples showed less than 10% degradation. If necessary, spectra were collected from photosensitive samples by collecting the spectrum in a 100-nm increment and then putting a fresh sample into the instrument. A detailed description of the laser flash photolysis apparatus has been published.<sup>5</sup>

Fluorescence quantum yields were determined using the actinometry method previously described.<sup>5</sup> Quinine sulfate was used as an actinometer with a known fluorescence quantum yield of 0.55 in 1.0 N H<sub>2</sub>SO<sub>4</sub>.<sup>14</sup> To minimize the contribution of phosphorescence to the emission spectrum, all samples were measured under air-saturated conditions and excited at 350 nm (325 nm for **half-PE1-Pt**) with a matched optical density of 0.1.

### Results and Discussion

Figure 2 summarizes IR and <sup>13</sup>C NMR data from **half-PEn-Pt** and **PEn-Pt**. The acetylenic Pt-C<sub>1</sub>≡C<sub>2</sub> stretch frequency

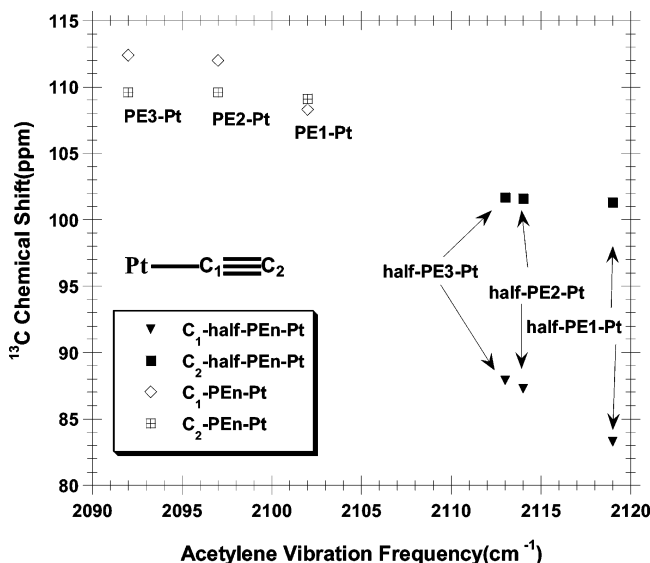


Figure 2. Summary of  $^{13}\text{C}$  NMR and IR data for the acetylenic carbons.

of **PE<sub>n</sub>-Pt** ranges from 2092 to 2102  $\text{cm}^{-1}$ , while that of **half-PE<sub>n</sub>-Pt** ranges from 2113 to 2119  $\text{cm}^{-1}$ . The lower frequency in **PE<sub>n</sub>-Pt** reflects back-bonding from Pt 5d orbital to the ligand's lowest-unoccupied molecular orbital (LUMO), lowering the bond order.<sup>15</sup> The vibration frequency observed in **half-PE<sub>n</sub>-Pt** is in the range of monosubstituted acetylenes.<sup>16</sup> The  $^{13}\text{C}$  NMR chemical shifts of **PE<sub>n</sub>-Pt** of C<sub>1</sub> and C<sub>2</sub> range from 108.3 to 112.4 ppm and from 109.1 to 109.6 ppm, respectively. In contrast, the shifts of **half-PE<sub>n</sub>-Pt** in C<sub>1</sub> and C<sub>2</sub> range from 83.3 to 87.9 ppm and from 101.3 to 101.7 ppm. The large downfield shift in **half-PE<sub>n</sub>-Pt** results from lower electron density on the terminal acetylene, especially in C<sub>1</sub>. These changes in the ground-state charge distribution result from the electron-withdrawing effect of the chlorine atom in **half-PE<sub>n</sub>-Pt**.

The ground-state absorption spectra of platinum acetylide complexes are  $\pi\pi^*$  transitions with metal-to-ligand charge transfer (MLCT) character.<sup>12</sup> The highest-occupied molecular orbital (HOMO) consists of  $\pi$  orbitals on the acetylene and aromatic groups with contribution from the 5d<sub>xy</sub> orbital on the platinum, while the LUMO consists of  $\pi^*$  orbitals with no contribution from the platinum.<sup>10,17</sup> Both the HOMO and LUMO are delocalized across the platinum. We previously found in the **PE<sub>n</sub>-Pt** complexes that, as the size of the ligand increased, the  $\pi\pi^*$  character of the optical transitions increased.<sup>5</sup> By assumption of  $D_{2h}$  symmetry, the most intense optical transition is a HOMO to LUMO ( $b_{2g}$  configuration  $\rightarrow$   $b_{3u}$  configuration) transition to the B<sub>1u</sub> state polarized parallel to the molecular axis.<sup>18</sup> Similarly, the **half-PE<sub>n</sub>-Pt** complexes have  $C_{2v}$  symmetry. In this case, the HOMO to LUMO ( $b_1$  configuration  $\rightarrow$   $b_1$  configuration) transition to the A<sub>1</sub> state will also be polarized along the molecular axis. The symmetry argument predicts the ground-state absorption spectra of the **half-PE<sub>n</sub>-Pt** complexes will be blue-shifted from their **PE<sub>n</sub>-Pt** counterparts. Figure 3 and Table 1 give ground-state absorption spectra data of **half-PE<sub>n</sub>-Pt** in comparison with those of **PE<sub>n</sub>-Pt** in benzene. For all three ligands, the ground-state absorption spectrum of **half-PE<sub>n</sub>-Pt** is blue-shifted from that of **PE<sub>n</sub>-Pt**. These results give evidence the S<sub>0</sub> and S<sub>1</sub> states are delocalized across the central platinum atom.

The spectra of all the complexes in Figure 3 contain at least two overlapping bands. Comparison of the band shapes for **half-PE2-Pt** vs **PE2-Pt** and **half-PE3-Pt** vs **PE3-Pt** show a

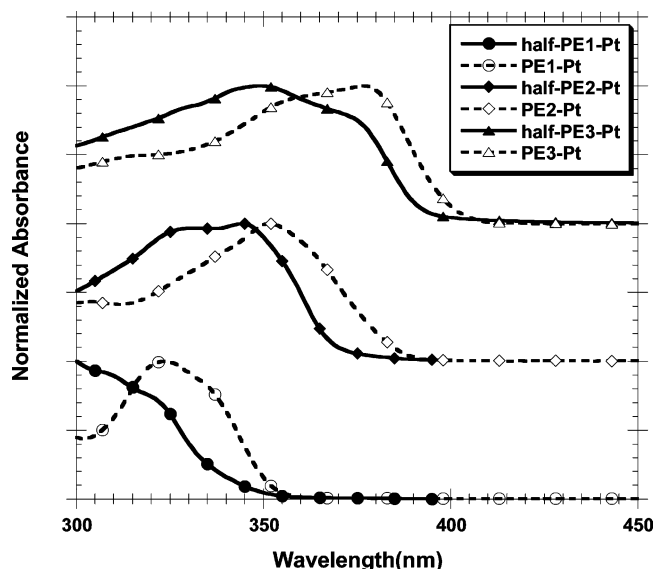


Figure 3. Ground-state absorption spectra of samples in benzene.

TABLE 1: Summary of Ground State Absorption Spectra Data

compound	absorbance ( $\lambda_{\text{max}}$ , nm)	extinction coefficient ( $\text{M}^{-1} \text{cm}^{-1}$ )	oscillator strength <sup>b</sup>
half-PE1-Pt	309(sh)	12 170 (700) <sup>a</sup>	0.31 <sup>c</sup>
half-PE2-Pt	344	53 600 (6600)	1.33
half-PE3-Pt	350	60 800 (2500)	1.83
PE1-Pt	324	24 700 (500)	0.63
PE2-Pt	355	89 000 (1200)	1.95
PE3-Pt	377	85 200 (1800)	2.25

<sup>a</sup> Number in parentheses is the standard deviation. Spectra were measured in benzene. <sup>b</sup> Oscillator strength was determined by fitting the absorption spectrum to three Gaussians and calculating the area.<sup>25</sup> <sup>c</sup> The oscillator strength for **half-PE1-Pt** was estimated from the ratio of its extinction coefficient to that of **PE1-Pt**.

difference between asymmetric and symmetric complexes. As the ground-state absorption spectra have MLCT character, the S<sub>1</sub> state will be similar to the LUMO of the ligand. Published investigations of the excited states of phenyl acetylene and diphenyl butadiyne provide insight into the ligand excited state. The spectroscopic properties of the asymmetric complexes are similar to phenylacetylene, where the aromatic rings of the LUMO have a quinone-like structure and the acetylene  $\pi^*$  orbitals are antibonding.<sup>19,20</sup> The ground-state spectrum band shape results from molecular vibrations in the LUMO, including C $\equiv$ C and C=C stretch modes. Similarly, the ground-state absorption spectrum of diphenyl butadiyne is a model of symmetric complexes.<sup>21,22</sup> As in phenyl acetylene, the aromatic rings become quinone-like and the terminal acetylene  $\pi^*$  orbitals become antibonding. The excited-state vibrations are similar to those seen in diphenyl butadiyne, where C $\equiv$ C and C=C stretch modes have been reported. Finally, The S<sub>1</sub> state of **PE1-Pt** has been shown to be ligand-centered with quinone-like aromatic rings and antibonding acetylene  $\pi^*$  orbitals.<sup>13</sup> On the basis of these results, the overlapping bands have vibronic contributions. The relative intensity of the bands reverses upon going from **PE<sub>n</sub>-Pt** to **half-PE<sub>n</sub>-Pt**. For example, in **PE2-Pt** I(361 nm)/I(352 nm) = 1.20, while in **half-PE2-Pt** I(345 nm)/I(330 nm) = 1.03. Similarly, in **PE3-Pt** I(377)/I(360) = 1.09, while in **half-PE3-Pt** I(371 nm)/I(350 nm) = 0.80. The changes in band shape suggest a decrease in 0–0 band intensity and increase in 0–1, 0–2, etc. intensity in the **half-PE<sub>n</sub>-Pt** complexes. The S<sub>1</sub>



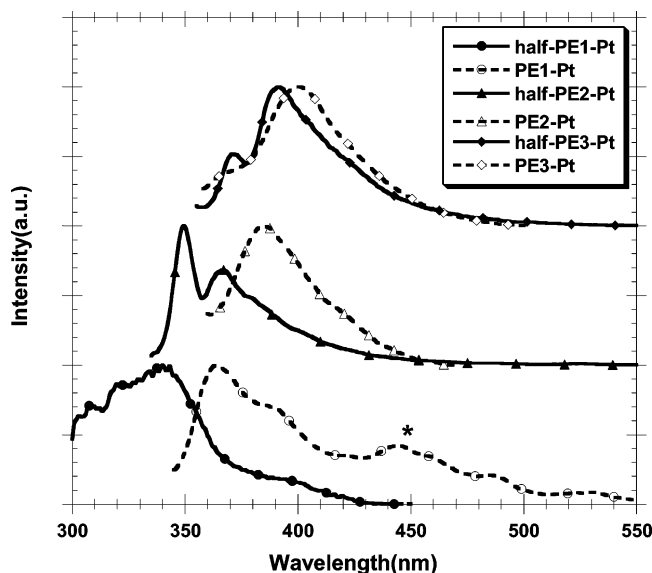


**Figure 4.** Fluorescence spectra. All samples are in benzene and excited at 290 nm (**half-PE1-Pt**), 325 nm (**PE1-Pt** and **half-PE2-Pt**), or 350 nm (**PE2-Pt**, **half-PE3-Pt** and **PE3-Pt**). Emission marked with asterisk is room-temperature phosphorescence of **PE1-Pt**.

**TABLE 2: Summary of Fluorescence and Phosphorescence Data**

compound	$\lambda_{\text{max}}^{\text{f}}$ (nm) <sup>a</sup>	$\phi_{\text{f}}$	$E_{\text{S}}$ (eV)	$\lambda_{\text{max}}^{\text{p}}$ (nm) <sup>b</sup>	$E_{\text{T}}$ (eV)	$\Delta E_{\text{ST}}$ (eV)
half-PE1-Pt	349	0.004	3.91	435	2.82	1.09
half-PE2-Pt	367	0.009	3.56	524	2.39	1.16
half-PE3-Pt	391	0.088	3.30	552	2.28	1.02
PE1-Pt	364	<0.0006	3.58	435	2.82	0.76
PE2-Pt	385	0.001	3.29	527	2.38	0.91
PE3-Pt	400	0.016	3.21	557	2.26	0.95

<sup>a</sup> Fluorescence spectra collected in benzene. <sup>b</sup> Phosphorescence spectra collected in Me-THF at 77 °K.

state is delocalized across the Pt in **PE<sub>n</sub>-Pt** but is confined to one ligand in **half-PE<sub>n</sub>-Pt**. The changes in band shape give evidence for a more distorted  $S_1$  state in **half-PE<sub>n</sub>-Pt**. As discussed below, similar changes in band shape occur in the phosphorescence spectrum.<sup>6,7</sup> Although the intensity ratio effects probably result from excited state geometry differences, the oscillator strengths approaching 2 in the larger complexes suggest the presence of more than one strongly allowed electronic transition in the ground-state absorption spectrum.

For a series of chromophores which consist of a number of repeat units, the oscillator strength and extinction coefficient of the ground-state absorption spectrum increases with chromophore length<sup>23</sup> but will be limited by conformation twisting effects.<sup>24</sup> The trend in the oscillator strength ratios is:  $f(\text{PE}_n\text{-Pt})/f(\text{half-PE}_n\text{-Pt}) = 2.0, 1.5$  and  $1.2$  for  $n = 1, 2,$  and  $3$ . If the  $S_1$  state were ligand-centered, the ratio would be 2.0 for all three types of chromophores. If the  $S_1$  state were delocalized across the platinum, the oscillator strength would also increase with length, but the ratio would not necessarily be 2.0. We observe the latter trend, so the oscillator strength data is consistent with the  $S_1$  state being delocalized across the platinum.

Figure 4 and Table 2 give fluorescence spectra data of **half-PE<sub>n</sub>-Pt** and **PE<sub>n</sub>-Pt**. Emission from the  $S_1$  state occurs after solvent and molecular relaxation. As with the ground-state absorption spectra, the emission spectra of all the **half-PE<sub>n</sub>-Pt** complexes are blue-shifted from those of the **PE<sub>n</sub>-Pt** counterparts. From these results, we conclude the fluorescing  $S_1$  state is delocalized across the platinum atom.

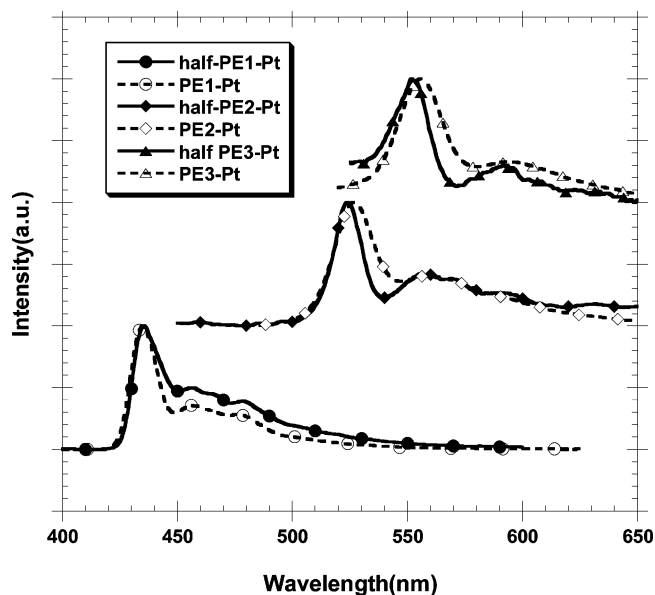


**Figure 5.** Phosphorescence spectra of complexes dissolved in a Me-THF glass at 77 K.

**TABLE 3: Summary of Triplet State Absorption Spectra Data**

compound	$T_1 - T_{n\lambda_{\text{max}}}$ (nm)	$E_{\text{Tmax}}$ (eV)
half-PE1-Pt	N/A <sup>a</sup>	N/A
half-PE2-Pt	570	2.18
half-PE3-Pt	620	2.00
PE1-Pt	630 <sup>b</sup>	1.97
PE2-Pt	586	2.12
PE3-Pt	640	1.94

<sup>a</sup> Unable to excite sample at 355 nm. <sup>b</sup> Data taken from ref 5.

For both **half-PE<sub>n</sub>-Pt** and **PE<sub>n</sub>-Pt**, the fluorescence quantum yield increases with ligand length. For a given ligand length, the quantum yield is 5–10× larger in **half-PE<sub>n</sub>-Pt**. The increase in quantum yield with ligand length has been attributed to the increasing  $\pi\pi^*$  character of the excited state with ligand length.<sup>5</sup> One factor influencing fluorescence quantum yield is the rigidity of the chromophore. The **PE<sub>n</sub>-Pt** chromophores have two ligands and the  $S_1$  state is delocalized across Pt atom. In contrast, the **half-PE<sub>n</sub>-Pt** chromophores have the  $S_1$  excited-state confined to one ligand. Twisting around the various bonds brings the  $S_1$  state to a geometry that allows for radiationless conversion to the ground state. There is more conformation flexibility (two acetylide ligands) in the **PE<sub>n</sub>-Pt** chromophores than in the **half-PE<sub>n</sub>-Pt** chromophores (one acetylide ligand). Rotation about the bonds promotes radiationless conversion to the ground state by providing a pathway for dissipation of excess thermal energy from the excited state, promoting increased radiationless decay and a lower fluorescence quantum yield.<sup>25</sup>

Figure 5 gives phosphorescence spectra of the **half-PE<sub>n</sub>-Pt** complexes and the **PE<sub>n</sub>-Pt** complexes dissolved in a glass. Table 2 gives additional phosphorescence data. If the  $T_1$  state is delocalized across the platinum, we would expect the phosphorescence spectra of the **half-PE<sub>n</sub>-Pt** complexes to be blue-shifted from those of the **PE<sub>n</sub>-Pt** complexes. In contrast to the ground-state absorption and fluorescence spectra described above, conversion of **PE<sub>n</sub>-Pt** to **half-PE<sub>n</sub>-Pt** results in virtually no difference in the emission spectra. Especially in **PE1-Pt** vs **half-PE1-Pt**, the 0–0 bands have nearly the same energy. There is a slight blue shift in **half-PE2-Pt** and **half-PE3-Pt**, suggesting a small amount of delocalization across the platinum. The phosphorescence spectra give evidence that the  $T_1$  state is nearly

entirely confined to one of the ligands. Similar behavior has been seen comparing the phosphorescence of  $\text{ClPt}(\text{PBu}_3)_2\text{C}\equiv\text{CC}_6\text{H}_4\text{C}\equiv\text{C}(\text{PBu}_3)_2\text{Cl}$  and the polymer  $(\text{Pt}(\text{PBu}_3)_2\text{C}\equiv\text{CC}_6\text{H}_4\text{C}\equiv\text{C})_n$ ,<sup>6</sup> as well as oligomers of increasing length.<sup>7</sup> The spectral shift of the triplet state 0–0 band upon conversion from monomer to polymer is very small, showing evidence of strong confinement of the triplet exciton. These results support published results suggesting the intersystem crossing process in **PE<sub>n</sub>-Pt** consists of the  $S_1$  state, having  $D_{2h}$  symmetry, being delocalized across the platinum atom, followed by movement of the  $T_1$  exciton to one ligand, having  $C_{2v}$  symmetry.<sup>10</sup> The intersystem crossing process has been proposed to occur by distortion along the  $B_{3u}$  antisymmetric stretch vibration mode, where the  $\text{C}\equiv\text{C}$  triple bond attached to the platinum stretches on one ligand and shortens on the other. The stretching stabilizes the  $\pi^*$  antibonding orbitals on one ligand and the shortening stabilizes the  $\pi$  bonding orbitals on the other ligand. The conical intersection between the singlet  $D_{2h}$  potential energy surface and the lower-energy triplet  $C_{2v}$  surface resides where one of the triple bonds is shortened and the other is lengthened. Upon spin flip, the triplet exciton resides on one ligand.

Additional evidence for symmetry changes during intersystem crossing comes from measurements of phosphorescence polarization in platinum acetylide polymers.<sup>18</sup> This study shows that the  $S_1$  state is polarized parallel to the molecular axis while the  $T_1$  state is polarized perpendicular to the molecular axis. The change in polarization results from spin–orbit–coupling–induced state mixing. The vibronic sidebands of the emission spectrum of **half-PE1-Pt** are more intense than those of **PE1-Pt**. This behavior is similar to a comparison of platinum acetylide monomer and polymer<sup>6</sup> and oligomers of increasing length<sup>7</sup> where a Huang–Rhys analysis of the vibronic sidebands shows more distortion of the  $T_1$  state vs the  $S_1$  state than the polymer. Even though the  $T_1$  state energy of **half-PE1-Pt** is the same as that of **PE1-Pt**, intersystem crossing from the **half-PE1-Pt**  $S_1$  state to the  $T_1$  state results in a more distorted  $T_1$  state. Because of the large fluorescent background in the phosphorescence spectra of **half-PE2-Pt** and **half-PE3-Pt**, we could not make band shape comparisons with the spectra of **PE2-Pt** and **PE3-Pt**.

The average singlet–triplet splitting  $\Delta E_{ST}$  for **half-PE<sub>n</sub>-Pt** is  $1.09 \pm 0.07$  eV, while it is  $0.87 \pm 0.10$  eV in **PE<sub>n</sub>-Pt**. This can be easily explained as the singlet–triplet splitting is proportional to the overlap integral between the two singly occupied molecular orbitals (SOMOs) of the triplet state. Both the  $\text{SOMO}_1$  and  $\text{SOMO}_2$  of the **half-PE<sub>n</sub>-Pt** chromophores are located on the half-chromophore. In contrast,  $\text{SOMO}_1$  and  $\text{SOMO}_2$  of **PE<sub>n</sub>-Pt** probably have some delocalization through the platinum atom into the other ligand. As a result, the overlap integral is larger in the **half-PE<sub>n</sub>-Pt** complexes, resulting in a larger  $\Delta E_{ST}$ .

Figure 6 and data from Table 3 show triplet state absorption spectra for **half-PE<sub>n</sub>-Pt** and **PE<sub>n</sub>-Pt**,  $n = 2$  or 3. Unlike the phosphorescence results described above, the triplet-state absorption spectra suggest that the  $T_n$  state is delocalized across the platinum center. The triplet state absorption spectrum of **PE2-Pt** is considerably broader than that of **half-PE2-Pt**. The phosphorescence data show that the  $T_1$  state is confined to one ligand of **PE2-Pt**. Clearly the  $T_n$  state of **PE2-Pt** is delocalized across the central platinum and well into the other ligand. The band shapes for **half-PE3-Pt** and **PE3-Pt** are similar. In our earlier work we showed the excited states of **PE<sub>n</sub>-Pt** have more  $\pi\pi^*$  character and platinum influence as  $n$  increases to 3.<sup>5</sup> The similarity in shape may say the  $T_n$  states of **half-PE3-Pt** and

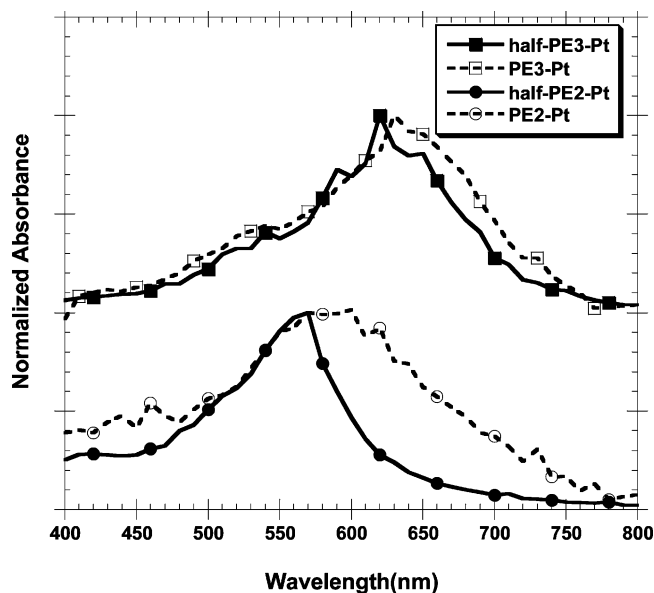


Figure 6. Triplet state absorption spectra in benzene for **half-PE<sub>n</sub>-Pt** and **PE<sub>n</sub>-Pt**,  $n = 2$  and 3.

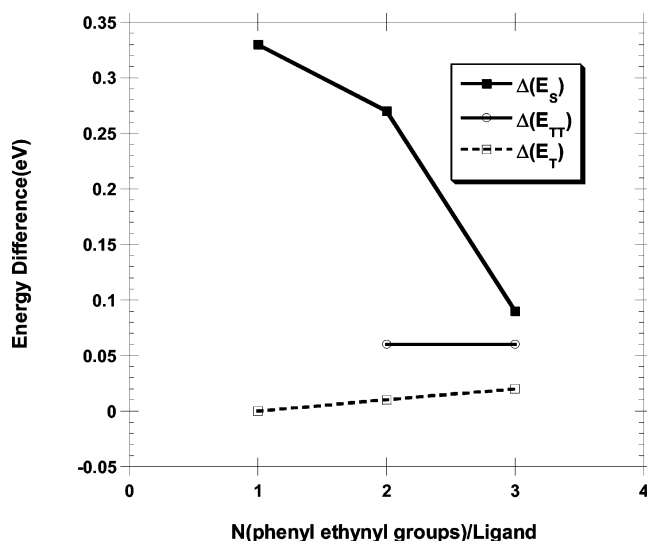
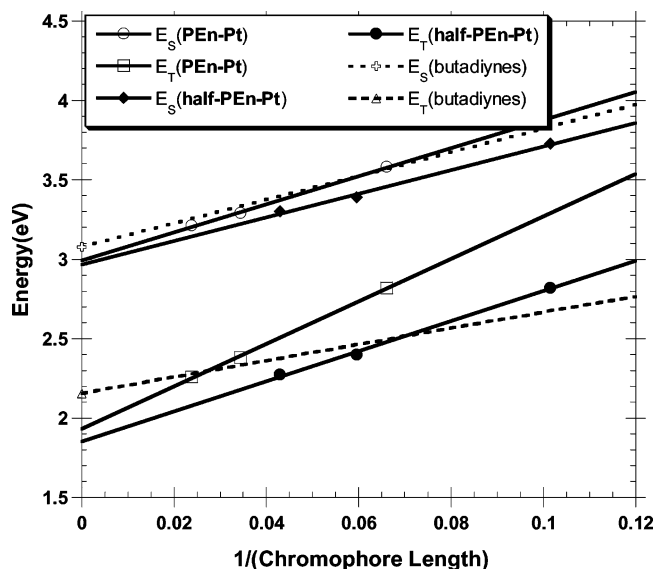


Figure 7. Plot of the state energy difference  $E(\text{half-PE}_n\text{-Pt}) - E(\text{PE}_n\text{-Pt})$  as a function of the number of phenyl ethynyl groups per ligand. Energies plotted are  $E_S$ ,  $E_T$ , and  $E_{TT}$ .

**PE3-Pt** have mostly  $\pi\pi^*$  character. For both  $n = 2$  and 3, the triplet state absorption spectrum of **half-PE<sub>n</sub>-Pt** is blue shifted compared to that of **PE<sub>n</sub>-Pt**. Theoretical calculations of the spatial extent of singlet and triplet excitons in platinum acetylide polymers have estimated the  $T_n$  exciton to be at least three repeating units in size.<sup>6</sup> The authors of that paper compare triplet state absorption spectra of the model compound  $\text{ClPt}(\text{PBu}_3)_2\text{C}\equiv\text{CC}_6\text{H}_4\text{C}\equiv\text{C}(\text{PBu}_3)_2\text{Cl}$  and the polymer  $(\text{Pt}(\text{PBu}_3)_2\text{C}\equiv\text{CC}_6\text{H}_4\text{C}\equiv\text{C})_n$ . They observe a large red shift upon conversion of the monomer to the polymer, again giving evidence the  $T_n$  state is delocalized across the platinum center. Polarized photoinduced absorption experiments have shown the  $T_1 - T_n$  transition is polarized parallel to the molecular axis.<sup>18</sup> As a result, the  $T_n$  state has ligand-to-metal charge-transfer character, with a contribution from the  $5d_{xz}$  orbital residing on the platinum center.

Figure 7 gives a plot of the state energy difference  $\Delta E = E(\text{half-PE}_n\text{-Pt}) - E(\text{PE}_n\text{-Pt})$  as a function of  $n$ . Energies plotted are  $E_S$ ,  $E_T$ , and  $E_{TT}$ . The largest effects appear for  $n = 1$ , with a substantial blue shift in  $\Delta E_S$ . The magnitude of the shift becomes smaller for  $n = 2$  and 3. This supports the idea



**Figure 8.** Plot of  $E_S$  and  $E_T$  vs the reciprocal of chromophore length ( $\text{\AA}^{-1}$ ). Also included for comparison are fitted lines for butadiynes and ligands.<sup>12</sup>

that the  $S_1$  state is delocalized across the platinum center in **PEn-Pt**. In comparison,  $\Delta E_T = 0$  for  $n = 1$  and is slightly positive for  $n = 2$  and 3. The  $T_1$  state is definitely confined to one ligand in **PE1-Pt**. In the other two types of chromophores there is slight delocalization across the platinum center. In our previous work we have shown the optical transitions of the **PEn-Pt** chromophores have mixed MLCT and  $\pi\pi^*$  character.<sup>5</sup> As the ligand size increases, the  $\pi\pi^*$  character increases. A possible explanation for this is spin-orbit-coupling-induced mixing of the  $T_1$  state with higher energy  $S_n$  states that are delocalized over the entire chromophore.<sup>18</sup> The energy difference  $\Delta E_{TT}$  does not change as  $n$  increases from 2 to 3, although, as shown in Figure 6, there are major bandwidth differences in the triplet state spectrum of **half-PE2-Pt** vs **PE2-Pt** not seen in **half-PE3-Pt** vs **PE3-Pt**. Because of the bandwidth changes,  $\Delta E_{TT}$  is not an accurate descriptor of the effect of  $n$  on the triplet state spectrum. An alternative descriptor is the energy shift at half-maximum. In this case, the energy shift is 0.23 eV for  $n = 2$  and 0.07 eV for  $n = 3$ , showing the  $T_n$  state is delocalized across the platinum atom.

In a previous publication we have shown a plot of  $E_S$  and  $E_T$  vs the reciprocal of end-to-end chromophore length gives a straight line.<sup>12</sup> The maximum conjugation length can be estimated from the intercept. Figure 8 shows a plot of  $E_S$  and  $E_T$  vs  $1/L$ .  $L$  is defined as the end-to-end chromophore length, calculated with Cambridgesoft Inc. Chem3D software. Because of the electron-withdrawing and possible conjugation effects of chlorine shown in Figure 2, the chromophore length of **half-PEn-Pt** included the default Pt-Cl bond length of 2.2905  $\text{\AA}$ . Also included in this plot is the regression line obtained previously from butadiynes and ligands.<sup>12</sup> Optical transitions in the butadiynes and ligands have  $\pi\pi^*$  character and can be used for comparison with the analogous platinum acetylides. The slope of the line measures the sensitivity of the state energy to increasing chromophore length, while the intercept estimates the state energy at large chromophore length. The  $E_S$  plots for **half-PEn-Pt** and **PEn-Pt** are very similar to that obtained from butadiynes and ligands. This suggests the  $S_1$  state of both **half-PEn-Pt** and **PEn-Pt** has the same dependence on length as the butadiynes and ligands, showing it is delocalized throughout the entire chromophore. The plots for the platinum complex's triplet state have larger slopes than found for the butadiynes

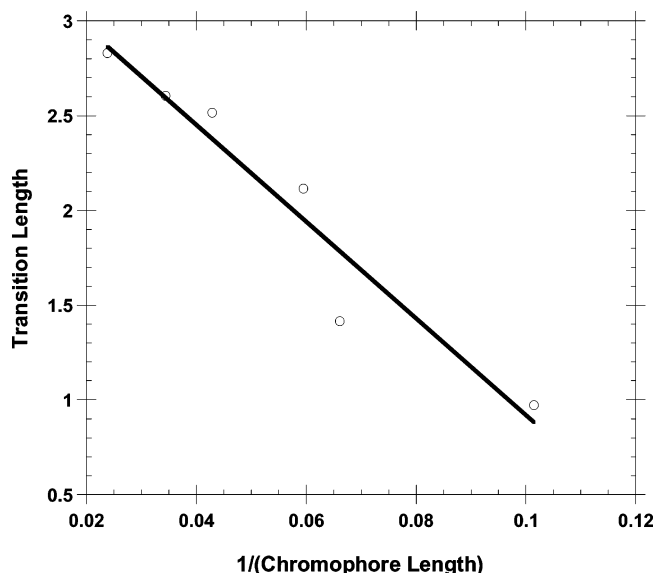


**Figure 9.** Plot of transition length ( $e \text{\AA}$ ) as a function of the reciprocal of chromophore length ( $\text{\AA}^{-1}$ ).

and ligands, showing a stronger sensitivity of  $E_T$  to chromophore length. The metal effects are largest in **half-PE1-Pt** and **PE1-Pt**, with small effects in the other platinum-containing chromophores. This result reflects the increased  $\pi\pi^*$  character of the excited states with larger ligands.

To find further evidence for delocalization of the singlet state through the platinum atom, we calculated the transition length from the oscillator strength<sup>25</sup>

$$f = \frac{8\pi^2 m_e}{3he^2} \nu M^2$$

The quantity  $\nu$  is the state energy in  $\text{cm}^{-1}$  and  $M$  is the transition length in  $e \text{\AA}$ . Figure 9 shows a plot of transition length as a function of  $1/L$  in the two types of chromophores. The linear behavior of the transition length parallels the trend in singlet state energy shown in Figure 8, giving further evidence the singlet state is delocalized across the platinum center.

In this article, we have compared the spectroscopic behavior of a series of **PEn-Pt** and **half-PEn-Pt** chromophores and have given evidence that the  $S_1$  and  $T_n$  states of the **PEn-Pt** chromophores are delocalized through the central platinum, while the  $T_1$  state is confined to one ligand. Published studies of the effect of conjugation length on  $S_1$  and  $T_1$  energies show variable results. Poly(thiophenes)<sup>26</sup> and carotenoids<sup>27</sup> with variable chromophore length have  $T_1$  states less sensitive to chromophore length than the  $S_1$  states. In contrast the  $T_1$  states in monodisperse  $\alpha$ -oligothiophenes<sup>28</sup> carbazole-spirobifluorene copolymers<sup>29</sup> and a homologous series of fluorene oligomers<sup>30</sup> have the same conjugation length dependence as the  $S_1$  states. Our previous paper<sup>12</sup> compares the chromophore length dependence for a series of platinum acetylide chromophores **PEn-Pt**, the corresponding ligands **PEn-H** and the butadiynes **PEn-BD**. The clearest trend appears for  $n = 1$ , where  $E_S(\text{PE1-H}) > E_S(\text{half-PE1-Pt}) > E_S(\text{PE1-BD}) > E_S(\text{PE1-Pt})$ , while  $E_T(\text{PE1-H}) > E_T(\text{half-PE1-Pt}) = E_T(\text{PE1-Pt}) > E_T(\text{PE1-BD})$ . The trend for  $E_S$  shows conjugation length increases with chromophore length. In contrast, the trend for  $E_T$  shows the platinum atom causes a break in the chromophore, confining the triplet exciton to one ligand. The trends for  $n = 2$  and 3 are less clear because the chromophore behavior becomes more strongly influenced by ligand length. Despite the ligand length effect,  $E_T(\text{half-PEn-}$

**Pt**)  $\approx E_T(\text{PE}_n\text{-Pt})$  for  $n = 2$  and  $3$ , showing the central platinum atom confines the triplet exciton to one ligand.

What causes the confinement of the triplet state in these systems? In general, the two electrons in the triplet state are not near each other as much as in the singlet state, resulting in less Coulombic repulsion.<sup>31</sup> An investigation of exciton mobility in platinum acetylide polymers had shown the rate of triplet exciton migration along the polymer chain is less than the rate of singlet exciton migration, suggesting the exciton migration time is longer than the triplet state lifetime.<sup>32</sup> The observation that during intersystem crossing the triplet state symmetry converts from  $D_{2h}$  to  $C_{2v}$  suggests the delocalized  $D_{2h}$  potential energy surface to be considerably higher in energy than the ligand-confined  $C_{2v}$  surface. After relaxation, the triplet exciton is confined in a  $C_{2v}$  symmetry potential energy well.<sup>10</sup> A recently published theoretical paper on **PE1-Pt** sheds more light on these issues.<sup>13</sup> They find the ground state to have  $D_{2h}$  symmetry, but the triplet state exciton has  $\pi\pi^*$  nature with the unpaired electron and hole delocalized over one phenylethynyl ligand. They calculate the barrier for the triplet exciton to hop to the other ligand to be 0.61 eV. This high-energy barrier will confine the exciton to one ligand.

**Acknowledgment.** The authors thank Jeff Skinn for spectroscopy measurements.

## References and Notes

- Cooper, T. M.; Hall, B. C.; Burke, A. R.; Rogers, J. E.; McLean, D. G.; Slagle, J. E.; Fleitz, P. A. *Chem. Mater.* **2004**, *16*, 3215–3217.
- Silverman, E. E.; Cardolaccia, T.; Zhao, X.; Kim, K.-Y.; Haskins-Glusac, K.; Schanze, K. S., *Coord. Chem. Rev.* **2005**, *249*, 1491–1500.
- Cooper, T. M. *Encyclopedia of Nanomaterials and Nanotechnology*; Nalwa, H. S., Ed.; American Scientific Publishers: 2004; Vol. 10, pp 447–470.
- Cooper, T. M.; McLean, D. G.; Rogers, J. E. *Chem. Phys. Lett.* **2001**, *349*, 31–36.
- Rogers, J. E.; Cooper, T. M.; Fleitz, P. A.; Glass, D. J.; McLean, D. G. *J. Phys. Chem. A* **2002**, *106*, 10108–10115.
- Beljonne, D.; Wittman, H. F.; Kohler, A.; S., G.; Younus, M.; Lewis, J.; Raithby, P. R.; Khan, M. S.; Friend, R. H.; Bredas, J. L. *J. Chem. Phys.* **1996**, *105*, 3868–3877.
- Liu, Y.; Jiang, S.; Glusac, K. D.; Powell, D. H.; Anderson, D. F.; Schanze, K. S. *J. Am. Chem. Soc.* **2002**, *124*, 12412–12413.
- Haskins-Glusac, K.; Ghiviriga, I.; Abboud, K. A.; Schanze, K. S. *J. Phys. Chem. B* **2004**, *108*, 4969–4978.
- Cooper, T. M.; Blaudeau, J.; Hall, B. C.; Rogers, J. E.; McLean, D. G.; Liu, Y.; Toscano, J. P. *Chem. Phys. Lett.* **2005**, *400*, 239–244.
- Emmert, L. A.; Choi, W.; Marshall, J. A.; Yang, J.; Meyer, L. A.; Brozik, J. A. *J. Phys. Chem. A* **2003**, *107*, 11340–11346.
- Jones, S. C.; Coropceanu, V.; Barlow, S.; Kinnibrugh, T.; Timofeeva, T.; Bredas, J. L.; Marder, S. R. *J. Am. Chem. Soc.* **2004**, *126*, 11782–11783.
- Rogers, J. E.; Hall, B. C.; Hufnagle, D. C.; Slagle, J. E.; Ault, A.; McLean, D. G.; Fleitz, P. A.; Cooper, T. M. *J. Chem. Phys.* **2005**, *122*, (21), 214701–214708.
- Batista, E. R.; Martin, R. L. *J. Phys. Chem. A* **2005**, *109*, 9856–9859.
- Demas, J. N.; Crosby, G. A. *J. Phys. Chem.* **1971**, *75*, 991–1022.
- Crabtree, R. H. *The Organometallic Chemistry of the Transition Metals*; John Wiley and Sons: New York, 2001.
- Silverstein, R. M.; Bassker, G. C.; Morrill, T. C. *Spectrometric Identification of Organic Compounds*; John Wiley and Sons: New York, 1974.
- Cooper, T. M.; Hall, B. C.; McLean, D. G.; Rogers, J. E.; Burke, A. R.; Turnbull, K.; Weisner, A.; Fratini, A.; Liu, Y.; Schanze, K. S. *J. Phys. Chem. A* **2005**, *109*, 999–1007.
- Wilson, J. S.; Wilson, R. J.; Friend, R. H.; Kohler, A.; Al-Suti, M. K.; Al-Mandhary, M. R. A.; Khan, M. S. *Phys. Rev. B* **2003**, *67*, 125206.
- Serrano-Andres, L.; Merchan, M. *J. Chem. Phys.* **2003**, *119*, 4294–4304.
- Amatatsu, Y.; Hasebe, Y. *J. Phys. Chem. A* **2003**, *107*, 11169–11173.
- Hoshi, T.; Okubo, J.; Kobayashi, M.; Tanizaki, Y. *J. Am. Chem. Soc.* **1986**, *108*, 3872–3879.
- Nagano, Y.; Ikoma, T.; Akiyama, K.; Tero-Kubota, S. *J. Am. Chem. Soc.* **2003**, *125*, 14103–14112.
- Yamabe, T.; Akagi, K.; Matsui, T.; Fukui, K.; Shirakawa, H. *J. Phys. Chem.* **1982**, *86*, 2365–2369.
- Crisp, G. T.; Bubner, T. P. *Tetrahedron* **1997**, *53*, 11881–11898.
- Turro, N. J. *Modern Molecular Photochemistry*; University Science Books: Sausalito, 1991.
- Monkman, A. P.; Burrows, H. D.; Hamblett, I.; Navarathnam, S.; Svensson, M.; Andersson, M. R. *J. Chem. Phys.* **2001**, *115*, 9046–9049.
- Rondonuwu, F. S.; Watanabe, Y.; Fujii, R.; Koyama, Y. *Chem. Phys. Lett.* **2003**, *376*, 292–301.
- Melo, J. S. d.; Silva, L. s. M.; Arnaut, L. s. G.; Becker, R. S. *J. Chem. Phys.* **1999**, *111*, 5427–5433.
- Rothe, C.; Brunner, K.; Bach, I.; Heun, S.; Monkman, A. P. *J. Chem. Phys.* **2005**, *122*, 084706–084712.
- Wasserberg, D.; Dudek, S. P.; Meskers, S. C. J.; Janssen, R. A. J. *Chem. Phys. Lett.* **2005**, *411*, 273–277.
- McGlynn, S. P.; Smith, F. J.; Cilento, G. *Photochem. Photobiol.* **1964**, *3*, 269–294.
- Haskins-Glusac, K.; Pinto, M. R.; Tan, C.; Schanze, K. S. *J. Am. Chem. Soc.* **2004**, *126*, 14964–14971.